LAWRENCE
LIVERMORE
NATIONAL
LABORATORY

LLNL-CONF-615495

ANALYSIS OF OPERATIONAL STRATEGIES FOR UTILIZING CO2 FOR GEOTHERMAL ENERGY PRODUCTION

T. A. Buscheck, M. Chen, C. Lu, Y. Sun, Y. Hao, M. A. Celia, T. R. Elliot, H. Choi, J. M. Bielicki

February 4, 2013

38th Workshop on Geothermal Reservoir Engineering
Stanford University, Palo Alto, CA, United States
February 11, 2013 through February 13, 2013

Disclaimer

PROCEEDINGS, Thirty-Eighth Workshop on Geothermal Reservoir Engineering
Stanford University, Stanford, California, February 11-13, 2013
SGP-TR-198

ANALYSIS OF OPERATIONAL STRATEGIES FOR UTILIZING CO_2 FOR GEOTHERMAL ENERGY PRODUCTION

Thomas A. Buscheck[1], Mingjie Chen[1], Chuanhe Lu[1], Yunwei Sun[1], Yue Hao[1], Michael A. Celia[2], Thomas R. Elliot[2], Hyungjin Choi[3], and Jeffrey M. Bielicki[3]

[1]Lawrence Livermore National Laboratory (LLNL)
P.O. Box 808, L-223, Livermore CA 94550, USA, e-mail: buscheck1@llnl.gov
[2]Department of Civil and Environmental Engineering, Princeton University, Princeton, NJ USA
[3]University of Minnesota, Minneapolis, MN USA

ABSTRACT

Geothermal energy production can be limited by insufficient working fluid and pressure depletion, whereas geologic CO_2 storage (GCS) can be limited by overpressure, which may drive CO_2 leakage and cause induced seismicity. Integration of these complementary systems can realize synergy, enhancing the viability of each system. While most research on CO_2-based geothermal systems has emphasized using CO_2 as a heat-transfer working fluid, it is possible to also use CO_2 as a supplemental pressure-support fluid to generate artesian pressures at the CO_2 and brine producers. A well pattern consisting of a minimum of four concentric rings of horizontal producers and injectors is proposed to conserve pressure from the injection process, minimize loss of CO_2, control the lateral extent of overpressure, and segregate the CO_2 and brine production zones. We present simulations of this approach for an idealized reservoir model, consisting of a relatively permeable sedimentary formation, confined by two impermeable confining units. Consideration of more realistic (heterogeneous) geologic settings and wellbore flow effects will be necessary to more rigorously evaluate the potential economic advantages of this approach.

INTRODUCTION

Economic viability of geothermal energy production requires a resource with high enough temperature, which will yield individual well flow rates sufficient to justify project development costs. Geothermal energy production can be limited by insufficient working fluid and pressure depletion. This depletion increases the parasitic cost of powering the fluid recirculation system, which can include the expense of submersible pumps. Sedimentary basins are often associated with low resource temperatures; however, such resources have the advantages of higher permeability, compared to typical hydrothermal systems, together with much of that being matrix (rather than fracture) permeability. Because of their high permeability, these basins may be used for geologic CO_2 storage (GCS). The NATCARB Regional Carbon Sequestration Partnership (RCSP) database (Carr et al., 2007) has identified extensive regions suitable for GCS. A significant subset of this area has high enough temperature to be of economic value for CO_2-based geothermal energy production (Elliot et al., 2013).

Geothermal energy production and GCS can contribute to lowering atmospheric CO_2 emissions, necessary for mitigating climate change (IPPC, 2005; Socolow and Pacala, 2006). For large-scale GCS, overpressure can limit the ability to store CO_2, while geothermal energy production can be limited by pressure depletion (Buscheck et al., 2012a; 2012b; 2012c). It is possible to synergistically integrate these systems, with CO_2 injection providing pressure support to maintain the productivity of geothermal brine producers, while the net loss of brine provides pressure relief and improved injectivity for CO_2 injectors.

Enhanced geothermal energy systems (EGS), a geothermal concept using CO_2 instead of water as the working fluid was first proposed by Brown (2000). Pruess (2006) followed up on his idea by analyzing reservoir behavior and found CO_2 to be superior to water in mining heat from hot fractured rock, including reduced parasitic power consumption to drive the fluid recirculation system. This concept has been extended to GCS in sedimentary formations (Randolph and Saar, 2011a; 2011b; 2011c; Saar et al., 2010), which they call a CO_2-Plume Geothermal (CPG) system, to distinguish it from CO_2-enabled EGS in crystalline rock. Because it is targeted for large, porous, permeable sedimentary basins, CPG can result in more CO_2 sequestration and more heat extraction than CO_2-based EGS in crystalline rock.

MULTI-RING WELL-PATTERN APPROACH

While most research on CO_2-based geothermal systems has emphasized using CO_2 as a working fluid (Pruess, 2006; Randolph and Saar, 2011a; 2011b, 2011c), it is possible to expand on this idea by using CO_2 as a pressure-support fluid to generate artesian pressures to drive both CO_2 and brine production. Initially, only brine is produced; however, as CO_2 breaks through to the producers, production transitions from brine to CO_2. Hence, this approach takes advantage of using both brine and CO_2 as working fluids. A key goal of this approach is for brine production rates (per well) to exceed the capacity of submersible pumps to take advantage of the large productivity of long-reach horizontal wells. This would provide greater leveraging of well costs, which would be particularly valuable for deep reservoirs.

For reasons discussed later, this approach requires a well pattern consisting of a minimum of four concentric rings of horizontal producers and injectors (Figure 1). The inner ring consists of brine/CO_2 producers and the second ring consists of CO_2 injectors. The third and fourth rings consist of brine reinjectors and producers, respectively. Each of these rings can include additional rings at different depths to provide better control of fluid and energy recovery for improved sweep efficiency, which would reduce thermal drawdown and increase project lifetime. This configuration can take advantage of the fact that horizontal-well drilling technology allows for precise directional control; hence, it is realistic to create precisely curved injection and production intervals.

The reason for using four concentric rings is to conserve pressure from injection operations and to minimize the loss of CO_2. This configuration implements a novel hydraulic ridge/divide strategy to assure only the inner-ring producers will ever extract CO_2, with the outer-ring producers only extracting brine (Figure 1). The outer ring creates a hydraulic trough to limit the lateral extent of overpressure, as well as to capture any CO_2 that may pass through the hydraulic ridge. This configuration spreads out overpressure to limit its magnitude, reducing the risks of induced seismicity and CO_2 leakage. An advantage of this approach is that storage of CO_2 displaces (and frees up) an equivalent volume of formation brine for recirculation. Because brine comes from the same formation, it reduces the possibility of chemical incompatibility, which could be an issue if brine came from a separate formation.

MODELING APPROACH

Reservoir analyses were conducted with the NUFT code, which simulates multi-phase heat and mass flow and reactive transport in porous media (Nitao, 1998). The pore and water compressibility are 4.5×10^{-10} and 3.5×10^{-10} Pa^{-1}, respectively. Water density is determined by the ASME steam tables (ASME, 2006). The two-phase flow of CO_2 and water was simulated with the density and compressibility of supercritical CO_2 determined by the correlation of Span and Wagner (1996) and viscosity determined by the correlation of Fenghour et al. (1997).

A generic system is modeled, consisting of a 250-m-thick reservoir with a permeability of 1×10^{-13} m^2, bounded by impermeable confining units with a permeability of 1×10^{-18} m^2. Hydrologic properties (Table 1) are similar to previous GCS and GCS-geothermal studies (Zhou et al., 2008; Buscheck et al., 2012a; 2012b; 2012c). Because conditions are laterally homogeneous, we can use a radially-symmetric (RZ) model. A geothermal gradient of 37.5°C/km and reservoir bottom depths of 2.5 and 5 km are considered. The RZ model is representative of rings of arc-shaped horizontal wells. Using an RZ model allows for fine mesh refinement, particularly around the injectors and producers to better model pressure gradients close to the wells. Gridblocks representing the injector and producer rings have dimensions similar to those of wellbores. All produced CO_2 is reinjected into the second ring and all produced brine is reinjected into the third ring. Initially, CO_2 injection rate is 480 kg/sec (15.2 MT/year), which is gradually increased to keep up with increasing CO_2 production.

Four- and five-ring well patterns of horizontal wells are considered. For the four-ring pattern, all of the wells are completed at the bottom of the reservoir (Figure 2). The inner production ring has a radius of 2 km. The second ring, representing CO_2 injectors, has a radius of 4 km. The third ring, representing brine injectors, has a radius of 6 km, and the fourth ring, representing brine producers, has a radius of 9 km. For the five-ring pattern, an additional inner ring of producers, with a radius of 1 km, is located in the upper portion of the reservoir (Figure 3). The purpose of the *upper* inner ring is to take advantage of the low density of CO_2 (compared to brine) and the influence of buoyancy, which will accelerate CO_2 breakthrough and increase its production and utilization as a working fluid for heat extraction. For the 2.5-km-deep reservoir, the bottomhole pressure of the producers is fixed to be 0.5 MPa greater than the ambient reservoir pressure at that depth. For the 5-km-deep reservoir, the bottomhole pressure of the producers is fixed to be 1.0 MPa greater than the ambient reservoir pressure at that depth. These assumed bottomhole pressures allow artesian flow up the well, while accounting for friction loss. Future reservoir analyses will include multi-phase wellbore models of brine and supercritical CO_2.

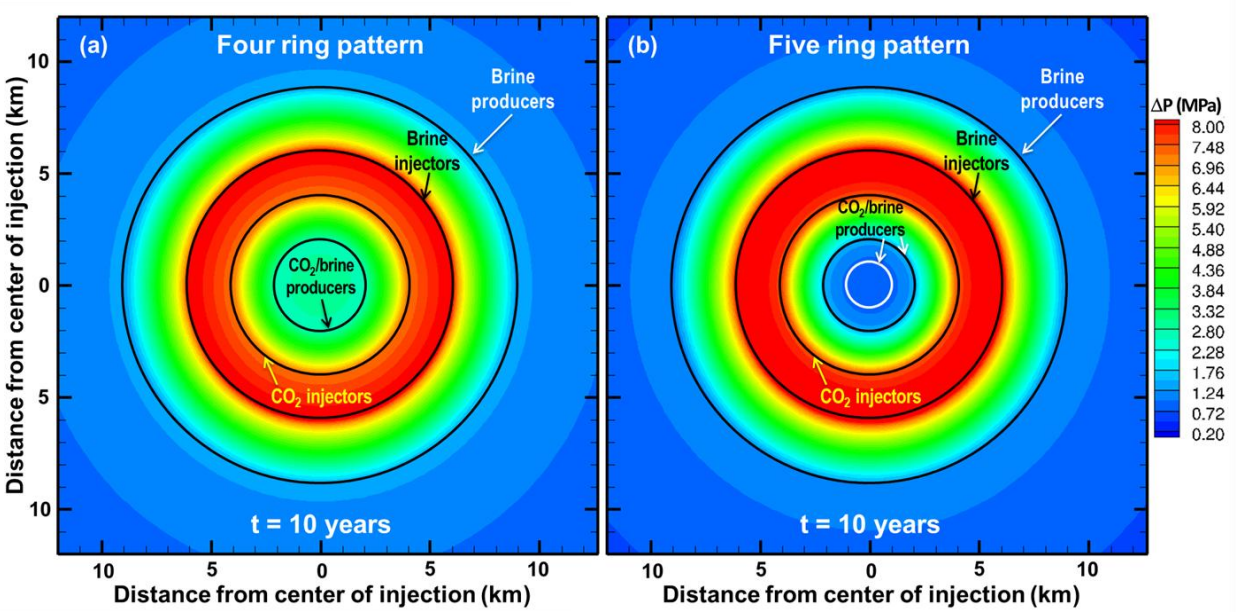

Figure 1: Overpressure ΔP at 10 years, at the elevation of the injectors and lower producers, for a reservoir bottom depth of 2.5 km for (a) four-ring horizontal-well pattern and (b) five-ring horizontal-well pattern.

Table 1: Hydrologic and thermal property values used in this study.

Property	**Reservoir**	**Confining units**
Permeability (m^2)	1.0×10^{-13}	1.0×10^{-18}
Thermal conductivity (W/m^oC)	2.0	2.0
Porosity	0.12	0.12
van Genuchten (1980) *m*	0.46	0.46
van Genuchten α (1/Pa)	5.1×10^{-5}	5.1×10^{-5}
Residual supercritical CO_2 saturation	0.05	0.05
Residual brine saturation	0.30	0.30

RESULTS

Four-ring well pattern, reservoir depth = 2.5 km

We start with the four-ring well pattern in a reservoir with a bottom depth of 2.5 km (Figures 1a, 2 and 4). A zone of maximum overpressure develops between the second ring of CO_2 injectors and the third ring of brine reinjectors (Figures 1a and 2a). This creates a hydraulic ridge/divide that restricts lateral migration of CO_2 (Figure 2b), thereby limiting the loss of CO_2, while conserving pressure buildup from CO_2 injection. The hydraulic ridge/divide segregates the CO_2- and brine-driven thermal plumes (Figure 2c and d), causing CO_2 to only be produced at the inner ring; with the outer ring only producing brine (Figure 4a). Initially, the inner ring only produces brine (Figure 4a), which is reinjected in the third ring. Because brine reinjection occurs in the zone of overpressure, driven by CO_2 injection (Figures 1a and 2a), it effectively drives flow "downhill" to the outer ring of producers, where it causes artesian flow. All brine produced in the outer ring is reinjected in the third ring. Overpressure and inner-ring brine production continue to increase for 8 years until CO_2 reaches the producers (Figure 4c). As CO_2 cut increases, inner-ring brine production decreases. Thus, there is less brine to be reinjected in third ring, which reduces the outer-ring brine production rate (Figure 4a). Note that the peak in outer-ring brine production lags slightly behind the peak for the inner producer ring.

All produced CO_2 is reinjected in the second ring. Because an important goal of this approach is to maximize the use of CO_2 as a working fluid, we continuously increased the CO_2 injection rate after CO_2 breakthrough (Figure 4a). Accordingly, the CO_2 injection rate was increased from an initial rate of 0.48 T/sec to greater than 4.0 T/sec. As the region between the first and second rings fills with CO_2, flow resistance between these rings is reduced, due to the low viscosity of CO_2, compared to brine. Thus, CO_2 delivery rate, which is the difference between the injection and production rates, declines from 15.2 MT/year to about 8 MT/year (Figure 4e). The reduction in CO_2 delivery rate decreases the rate at which net CO_2 storage accumulates, which is 373 and 1083 MT at 30 and 100 years, respectively (Figure 4e). As CO_2 cut increases, a greater fraction of produced

CO_2 is recirculated CO_2. At 20 years, 78 percent of produced CO_2 is recirculated, while 84, 90, and 92 percent of CO_2 production is recirculated at 30, 50, and 65 years, respectively (Figure 4f).

Thermal mixing causes an immediate small decline in extraction temperature, as cooler brine from the upper reservoir is drawn down to the producers at the bottom of the reservoir (Figure 4c). CO_2 breakthrough causes a small decline in extraction temperature at 8 years for the inner ring (Figure 4c). Because of the low heat capacity of CO_2, compared to brine, thermal drawdown is minimal until ~70 years. Because of the greater (3-km) spacing between the third and fourth (outer) rings, and because production rate per unit length of producer is less for the outer ring than it is for the inner ring, thermal drawdown is much less for the outer-ring producers.

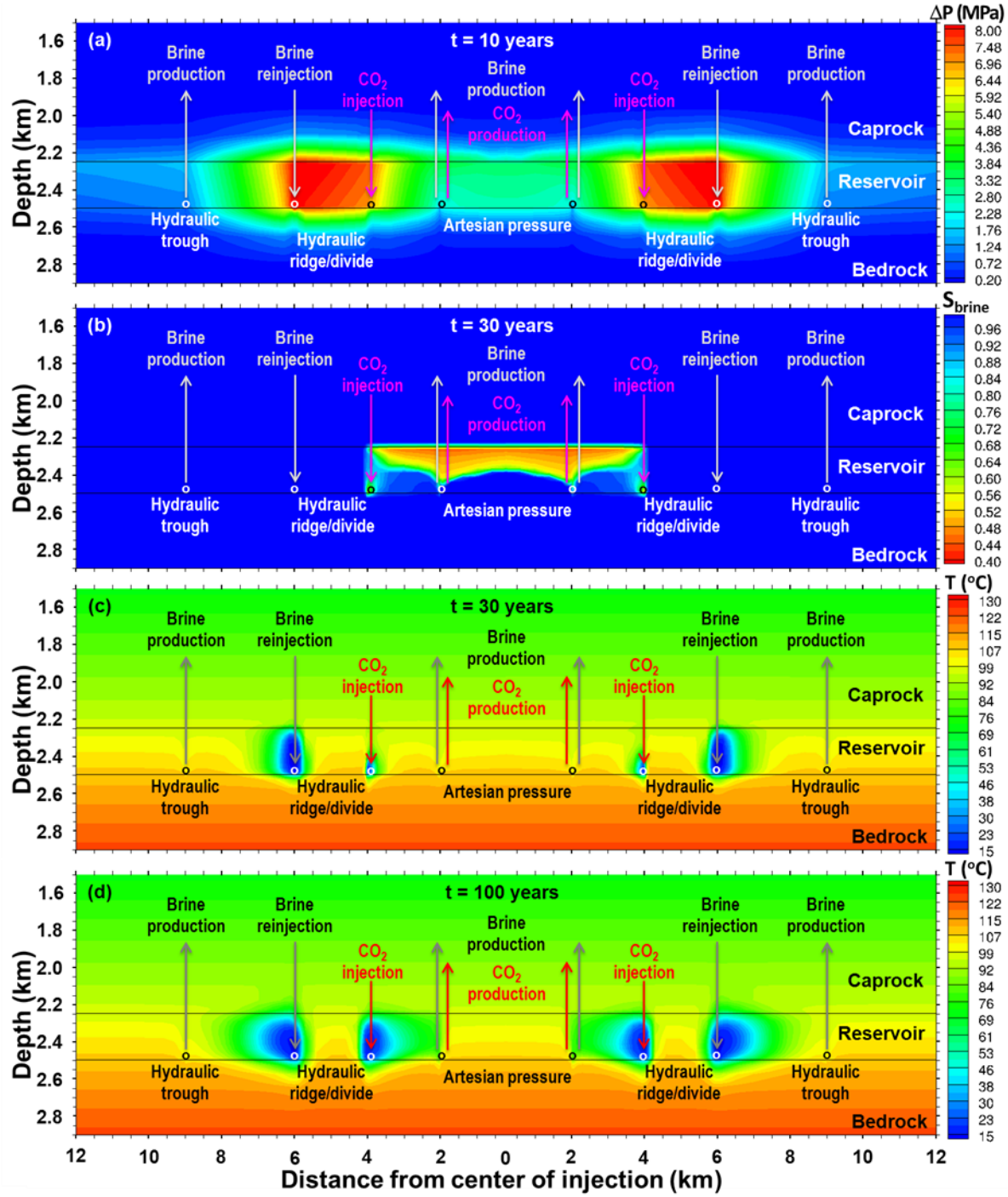

Figure 2: Four-ring pattern of horizontal wells, reservoir bottom depth of 2.5 km: (a) overpressure ΔP at 10 years, (b) brine saturation S_{brine} at 30 years, and (c,d) temperature T at 30 and100 years.

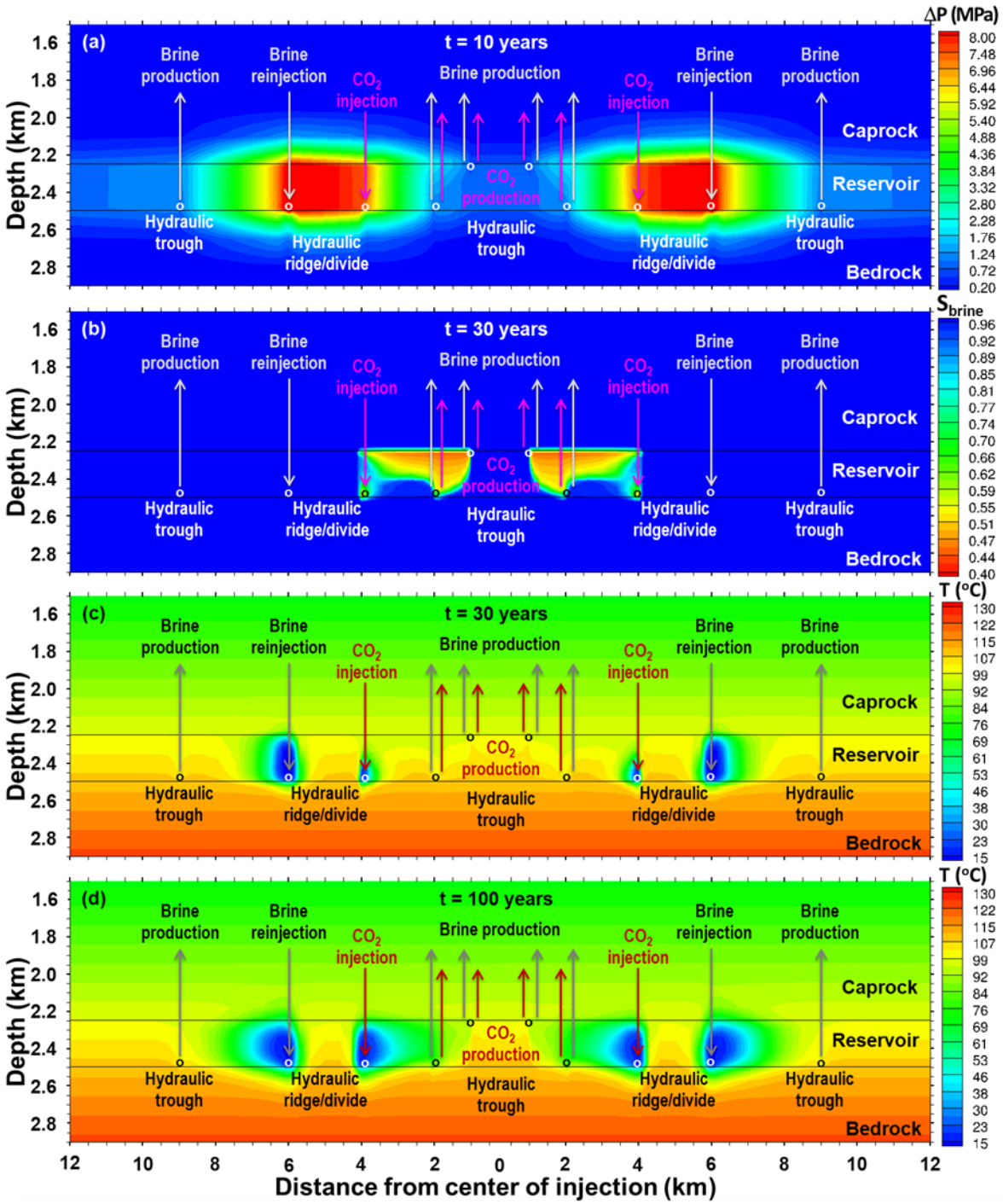

Figure 3: Five-ring pattern of horizontal wells, reservoir bottom depth of 2.5 km: (a) overpressure ΔP at 10 years, (b) brine saturation S_{brine} at 30 years, and (c,d) temperature T at 30 and100 years.

At 30 years, the thermal plumes have not reached the producers (Figure 2c). At 100 years, the inner thermal plume has reached the inner producers, while the outer thermal plume has not yet reached the outer producers (Figure 2d). Because thermal decline for brine production is negligible, the brine-based heat extraction rate exactly corresponds to the brine production rate for both the inner and outer producers (Figures 4a and b). CO_2-based heat extraction rate corresponds exactly with CO_2 production rate until the thermal decline becomes significant at ~70 years (Figures 4a, b, and c).

Power generation

Using GETEM (DOE, 2012), we built a binary-cycle net-power generation table for resource temperatures of 90, 100, 125, 150, 175, 200, and 225°C, and depths of 2.5 and 5 km, assuming submersible pumps are not

required. This table was used to create conversion efficiencies to convert from heat extraction rate to net-power generation, which were used to interpolate values of conversion efficiency corresponding to the simulated extraction temperatures. For CO_2-based, direct-turbine, power generation, we used a table of CO_2 system conversion efficiencies that include all losses in the entire power system, including pumps and cooling equipment (Randolph, 2013). After applying the brine and CO_2 conversion efficiencies to the respective heat extraction rates, we determine brine-based, CO_2-based, and total net power generation (Figure 4d). At early time, power is entirely generated from brine production. Starting at 8 years, CO_2-based power generation begins. The contribution of CO_2-based power increases with time until it is almost equal to brine-based power. Tables 2 and 3 summarize power generation for the first 30 and 100 years, respectively, including power sales, and power sales per MT of net CO_2 storage.

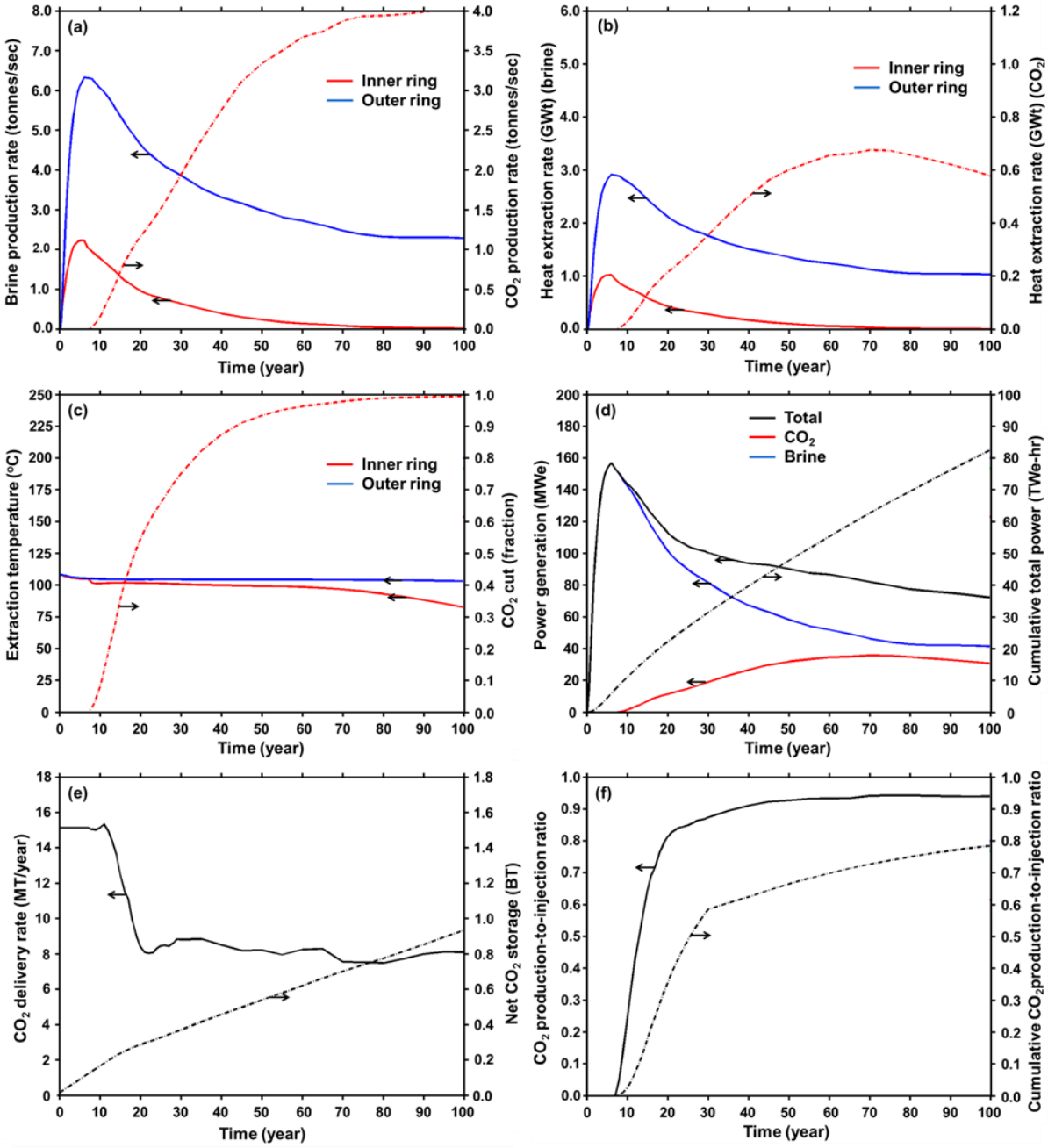

Figure 4: Four-ring pattern of horizontal wells, reservoir bottom depth of 2.5 km: (a) brine and CO_2 production rate, (b) brine- and CO_2-based heat extraction rate, (c) extraction temperature, (d) brine- and CO_2-based electrical power generation, (e) CO_2 delivery rate and net CO_2 storage, (f) instantaneous and cumulative ratio of CO_2 production to CO_2 injection.

Table 2: Summary of power generation for the first 30 years.

Well pattern	Reservoir depth (km)	Total energy (brine) (kW-hr)	Total energy (CO_2) (kW-hr)	Total energy (brine+CO_2) (kW-hr)	Total sales @ 10¢/kW-hr (M$)	Net storage (CO_2) (MT)	$/MT ($CO_2$)	Average power (MWe)	Annual power sales (M$)
Four ring	2.5	2.94e10	2.01e9	3.14e10	3141	371	8.47	119.4	104.7
	5	1.09e11	4.34e9	1.13e11	11300	447	25.28	429.7	376.7
Five ring	2.5	3.26e10	3.44e9	3.60e10	3600	397	9.07	136.9	120.0
	5	1.15e11	7.16e9	1.22e11	12248	453	27.04	465.7	408.3

Table 3: Summary of power generation for the first 100 years.

Well pattern	Reservoir depth (km)	Total energy (brine) (kW-hr)	Total energy (CO_2) (kW-hr)	Total energy (brine+CO_2) (kW-hr)	Total sales @ 10¢/kW-hr (M$)	Net storage (CO_2) (MT)	$/MT ($CO_2$)	Average power (MWe)	Annual power sales (M$)
Four ring	2.5	6.09e10	2.17e10	8.26e10	8260	936	8.82	94.3	82.6
	5	2.55e11	8.18e10	3.36e11	33600	1264	26.58	383.3	336.0
Five ring	2.5	6.21e10	2.49e10	8.70e10	8700	860	10.12	99.2	87.0
	5	2.48e11	9.06e10	3.39e11	33900	1278	26.53	361.7	339.0

Five-ring well pattern, reservoir depth = 2.5 km

In the preceding example, CO_2 breakthrough and production is delayed, in part, because the inner producers were located at the bottom of the reservoir. To promote earlier CO_2 breakthrough and production, we consider a five-ring pattern of horizontal wells, at the same reservoir bottom depth (2.5 km). This case is the same as the four-ring case, with the addition of an inner ring of producers at the top of the reservoir (Figures 1a and 3). CO_2 breakthrough occurs at just 5 years (Figure 5c), compared to 8 years in the 4-ring case. Earlier CO_2 breakthrough reduces brine production at the upper inner ring (Figure 5a). CO_2 production at the upper inner ring also reduces overpressure in the center of the reservoir (compare Figure 1b with 1a and Figure 3a with 2a), where it also prevents CO_2 storage (compare Figure 3b with 2b). The additional inner ring also increases inner-ring brine production, which increases the brine reinjection and outer-ring brine production rates. Increased CO_2 production reduces the CO_2 delivery rate and net CO_2 storage (compare Figure 5e with 4e). The ratio of produced to injected CO_2 is also increased (compare Figure 5f with 4f). The five-ring case generates more brine-based power, CO_2-based power, and total power, as well as more power sales per MT of net CO_2 storage (Tables 2 and 3).

Four-ring well pattern, reservoir depth = 5 km

We also considered the four- and five-ring cases for a reservoir bottom depth of 5 km (Figures 6 and 7). Because water viscosity decreases more steeply with temperature than does that of supercritical CO_2, the CO_2-to-brine mobility ratio decreases with temperature. This causes preferential CO_2 flow to be less pronounced at higher temperature, which delays CO_2 breakthrough and causes CO_2 cut to increase more slowly (compare Figure 6c with 4c). Reduced recirculation of previously produced CO_2 causes CO_2 delivery rate to remain high, increasing net CO_2 storage (compare Figure 6e with 4e) and reducing CO_2 production to injection ratio (compare Figure 6f with 4f). Reduced preferential flow of CO_2 also slows down thermal drawdown for the inner producers (compare Figure 6c with 4c). The larger volume of stored CO_2 displaces more brine, which increases brine production and reduces the rate of decline (compare Figure 6a with 4a). Thus, brine-base heat extraction remains high for 100 years (Figure 6b). Reduced thermal drawdown allows CO_2-based heat extraction to remain high. It is worth noting that increasing the reservoir bottom depth from 2.5 to 5 km, increases power generation by factors of 3.6 and 4 for 30 and 100 years, respectively, and triples power sales per MT of net CO_2 storage (Tables 2 and 3).

Five-ring well pattern, reservoir depth = 5 km

For a reservoir bottom depth of 5 km, the addition of the upper inner producer ring promotes earlier CO_2 breakthrough (compare Figure 7c with 6c), while increasing CO_2 production (compare Figure 7a with 6a). Thermal drawdown is negligible for the upper inner and outer producer rings (Figure 7c). For the lower inner producer ring, thermal drawdown is slower than it was for the five-ring case with a depth of 2.5 km (compare Figure 7c with 5c). For the upper inner and outer producer rings, negligible thermal drawdown allows the heat extraction history to almost exactly coincide with the corresponding fluid production history. The modest thermal drawdown starting around 70 years for the lower inner producer ring causes CO_2-

based heat extraction to decline slightly. Increasing the depth from 2.5 to 5 km, triples the power sales per MT of stored CO_2 for the five-ring cases, as it did for the four-ring cases (Tables 2 and 3).

During the first 30 years, the addition of the upper inner ring has a large effect, increasing brine-based power by 11 and 6 percent for the 2.5 and 5 km depths, respectively, while increasing CO_2-based power by a factor of 2.2 and by 65 percent (Table 2). Over a 100-year period, adding the upper inner ring has a smaller effect; reducing brine-based power by 3 percent, while increasing CO_2-based power by 11 percent (Table 3). Over a 100-year period, CO_2-based power is 26 and 24 percent of total power for the four-ring cases with 2.5 and 5 km depths respectively, while it is 29 and 27 percent of total power for the five-ring cases with 2.5 and 5 km depths, respectively (Table 3).

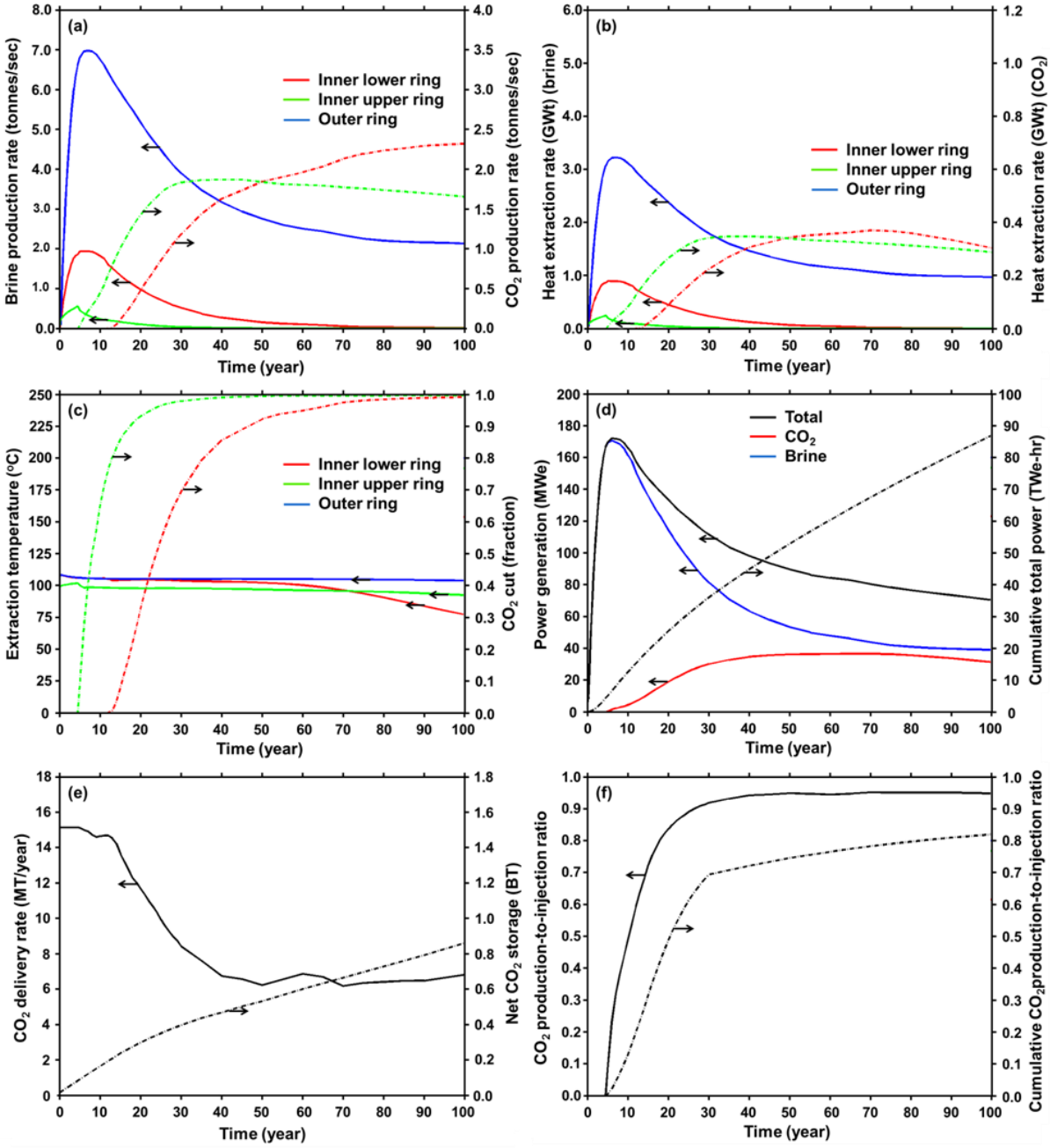

Figure 5: Five-ring pattern of horizontal wells, reservoir bottom depth of 2.5km: (a) brine and CO_2 production rate, (b) brine- and CO_2-based heat extraction rate, (c) extraction temperature, (d) brine- and CO_2-based electrical power generation, (e) CO_2 delivery rate and net CO_2 storage,(f) instantaneous and cumulative ratio of CO_2 production to CO_2 injection.

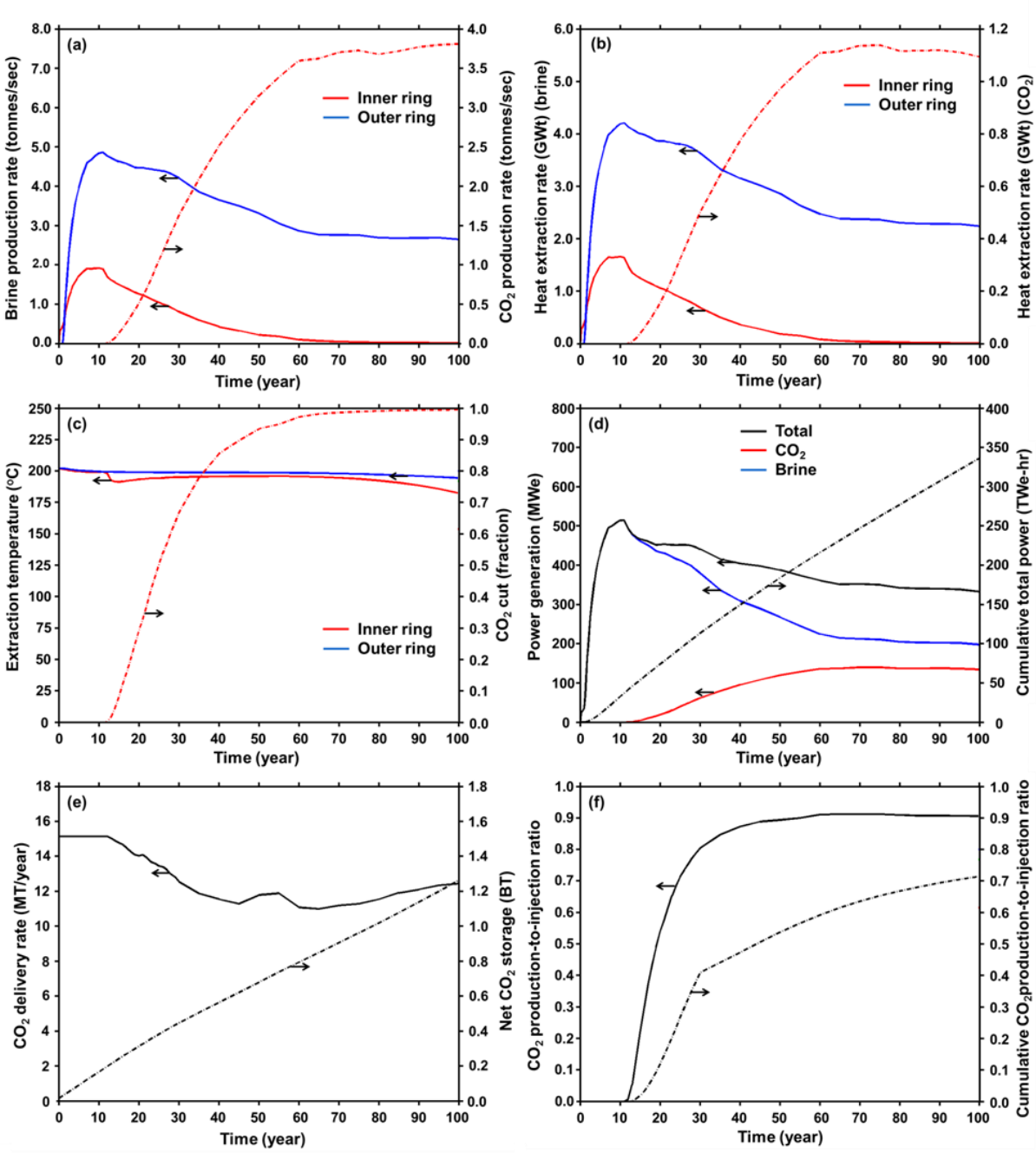

Figure 6: Four-ring pattern of horizontal wells, reservoir bottom depth of 5 km: (a) brine and CO_2 production rate, (b) brine- and CO_2-based heat extraction rate, (c) extraction temperature, (d) brine- and CO_2-based electrical power generation, (e) CO_2 delivery rate and net CO_2 storage, (f) instantaneous and cumulative ratio of CO_2 production to CO_2 injection.

Reservoir pressure

Maximum overpressure always occurs between the CO_2 injectors and brine reinjectors (Figures, 1, 2a, and 3a). Overpressure continues to increase until CO_2 reaches the inner producers. Because the five-ring pattern promotes earlier CO_2 breakthrough, peak overpressure is less (Figure 1). Because CO_2 and water viscosity decrease with temperature, hydraulic conductivity is greater for the reservoir bottom depth of 5 km than it is for a depth of 2.5 km, resulting in lower peak overpressure. For the cases considered in this study, peak overpressure never exceeds 8 MPa, which is 32 and 16 percent of hydrostatic pressure for depths of 2.5 and 5 km, respectively; which is far below fracture overpressure (typically approximated as 80 percent of hydrostatic pressure).

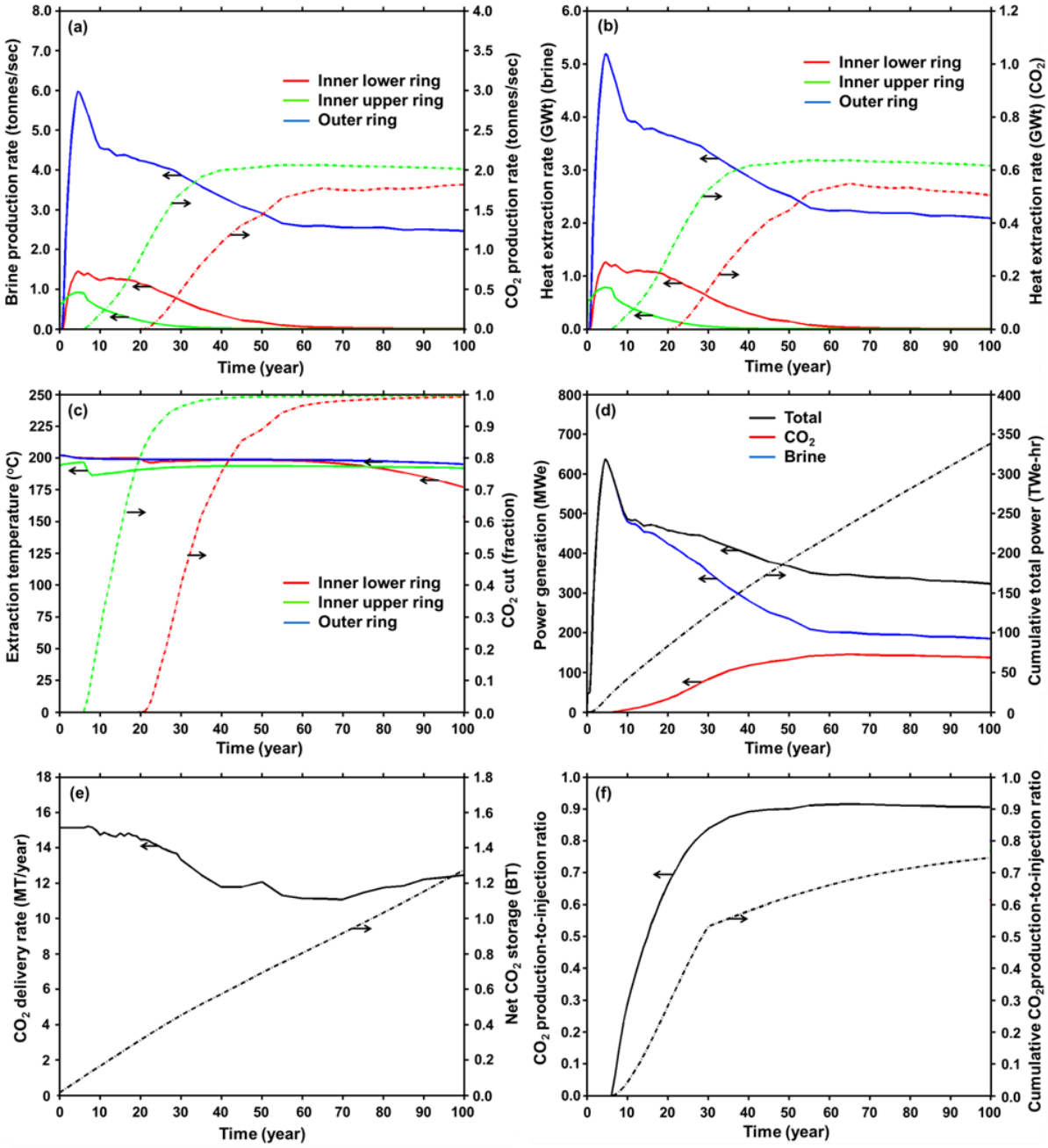

Figure 7: Five-ring pattern of horizontal wells, reservoir bottom depth of 5 km: (a) brine and CO_2 production rate, (b) brine- and CO_2-based heat extraction rate, (c) extraction temperature, (d) brine- and CO_2-based electrical power generation, (e) CO_2 delivery rate and net CO_2 storage, (f) instantaneous and cumulative ratio of CO_2 production to CO_2 injection.

FUTURE WORK

We present promising results for an innovative approach using CO_2 for pressure support to drive the recirculation of CO_2 and brine as working fluids, which could contribute to the next generation of geothermal energy production. We used a homogeneous model and future work should address the impact of realistic, heterogeneous geology and how this approach might be adapted to complex reservoir settings. Heterogeneity may result in earlier CO_2 breakthrough, which may increase the relative contribution of CO_2-based power, while decreasing the contribution of brine-based power. Heterogeneity may also reduce net CO_2 storage. To more rigorously determine the economic benefits of this approach, it will also be important to incorporate wellbore models of the multi-phase flow of CO_2 and brine. This will be important in assessing the potential

brine-production capacity of long-reach horizontal wells, driven by artesian pressures. The use of a wellbore model will also allow for a more rigorous assessment of the influence of the thermosyphon effect, together with that of artesian pressure, on CO_2-production capacity of horizontal wells.

CONCLUSIONS

Much of the research in applying supercritical CO_2 to geothermal power systems has focused on using CO_2 as a working fluid. This stems from the advantageous thermophysical properties of CO_2, which can reduce the parasitic costs of powering fluid recirculation and enable more direct and efficient power conversion through a turbine. In this paper, we expand upon this idea by demonstrating how CO_2 can be also used as a pressure-support fluid to generate artesian pressures to drive both brine and CO_2 production, thereby using both fluids as working fluids. We develop a well-pattern concept to address the following goals:

- Conserve pressure from injection operations to maximize the fluid-production benefit.
- Minimize the loss of CO_2.
- Manage overpressure to reduce related risks, such as induced seismicity and CO_2 leakage.
- Better control of fluid and energy recovery for improved sweep efficiency.
- Provide supplemental pressure-support and working fluids that are chemically compatible with the reservoir formation.

To meet these goals, we proposed and analyzed a well pattern consisting of a minimum of four concentric rings of horizontal producers and injectors, as follows:

1. Inner-ring brine/CO_2 producers
2. CO_2 injectors
3. Brine reinjectors
4. Outer-ring brine producers

For reservoir bottom depths of 2.5 and 5 km, we considered four- and five-ring well patterns, and find:

- A hydraulic ridge/divide is created that restricts lateral migration of CO_2, causing CO_2 production to only occur at the inner ring, while the outer ring only produces brine.
- Artesian pressures are created that drive large brine production rates, which generate power almost immediately, and provide a significant fraction of the total power.
- Because of the density difference between supercritical CO_2 and brine, the inclusion of production (and injection) intervals at multiple depths can enable better control of the relative rates of CO_2 and brine production, which can be a useful tool to improve sweep efficiency.
- After CO_2 breakthrough, CO_2-based power increases, while brine-based power decreases.
- Preferential CO_2 flow decreases with depth; thus, the fraction of produced CO_2 that is recycled decreases with depth, while net CO_2 storage increases.
- Increasing the reservoir bottom depth from 2.5 to 5 km quadruples power generation over a 100-year period, while power sales per MT of stored CO_2 is tripled.
- Net storage of CO_2 frees up an equivalent volume of make-up brine for reinjection, with the distinct advantage of being derived from the same formation, which reduces the possibility of chemical incompatibility.

The results of our study indicate that the multi-ring, horizontal-well approach, which uses CO_2 as both a pressure-support and working fluid, has the potential of improving the economic viability of geothermal energy production in sedimentary formations.

ACKNOWLEDGEMENT

This work was sponsored by the USDOE Geothermal Technologies Program, managed by Joshua Mengers, by the Carbon Mitigation Initiative at Princeton University, and by Ormat Technologies, under the direction of Ezra Zemach. We also acknowledge Jimmy Randolph at the University of Minnesota for providing the conversion efficiencies for power generated from direct CO_2 turbines. This work was performed under the auspices of the USDOE by LLNL under contract DE-AC52-07NA27344.

REFERENCES

ASME, 2006. ASME Steam Tables Compact Edition, ASME, Three Park Avenue, New York, NY, USA.

Brown, D.W., 2000. A hot dry rock geothermal energy concept using supercritical CO_2 instead of water. *Proceedings of the 25th Workshop on Geothermal Reservoir Engineering*, Stanford University, 233-238.

Buscheck, T.A., Sun, Y., Chen, M., Hao, Y., Wolery, T.J., Bourcier, W.L., Court, B., Celia, M.A., Friedmann, S.J., and Aines, R.D., 2012a. Active CO_2 reservoir management for carbon storage: Analysis of operational strategies to relive pressure buildup and improve injectivity, *Internationl Journal of Greenhouse Gas Control*, **6**, 230–245, doi:10.1.1016/j.ijggc.2011.11.007.

Buscheck, T.A., Elliot, T.R., Celia, M.A., Chen, M., Hao, Y., Lu, C., Sun, Y., 2012b. Integrated, geothermal-CO_2 storage reservoirs: adaptable, multi-stage, sustainable, energy-recovery strategies that reduce carbon intensity and environmental risk, *Proceedings for the Geothermal Resources Council 36th Annual Meeting*, 30 Sept–3 Oct, 2012, Reno, NV, USA.

Buscheck, T.A., Elliot, T.R., Celia, M.A., Chen, M., Sun, Y., Hao, Y., Lu, C., Wolery, T.J., and Aines, R.D., 2012c. Integrated geothermal-CO_2 reservoir systems: Reducing carbon intensity through sustainable energy production and secure CO_2 storage, *Proceedings of the International Conference on Greenhouse Gas Technologies (GHGT-11)*, Kyoto, Japan, 18–22 Nov, 2012.

Carr, T.R., Rich, P.M., and Bartley, J.D., 2007. The NATCARB geoportal: linking distributed data from the Carbon Sequestration Regional Partnerships. *Journal of Map and Geography Libraries: Special Issue on Department of Energy (DOE) Geospatial Science Innovations*, **4**, 131–147.

DOE, 2012. GETEM–Geothermal electricity technology evaluation model, August 2012 Beta, USDOE Geothermal Technologies Program.

Elliot, T.R., Buscheck, T.A., and Celia, M.A., 2013. Active CO_2 reservoir management for sustainable geothermal energy extraction and reduced leakage, *Greenhouse Gases: Science and Technology*, **1**, 1–16; DOI: 1002/ghg.

Fenghour, A., Wakeham, W.A., and Vesovic, V., 1998. The viscosity of carbon dioxide. *J. Phys. Chem. Ref. Data*, **27** (1), 31–44.

IPPC (Intergovermental Panel on Climate Change), 2005. Special report on carbon dioxide capture and storage. Cambridge University Press, Cambridge, UK and New York, NT, USA.

Nitao, J.J., 1998. "Reference manual for the NUFT flow and transport code, version 3.0," Lawrence Livermore National Laboratory, UCRL-MA-130651-REV-1, Livermore, CA, USA.

Pruess, K., 2006. Enhanced geothermal systems (EGS) using CO_2 as working fluid–a novel approach for generating renewable energy with simultaneous sequestration of carbon, *Geothermics*, **35**, 351–367.

Randolph, J.B. and Saar, M.O., 2011a. Coupling carbon dioxide sequestration with geothermal energy capture in naturally permeable, porous geologic formations: Implications for CO_2 sequestration. *Energy Procedia*, **4**, 2206–2213.

Randolph, J.B. and Saar, M.O., 2011b. Impact of reservoir permeability on the choice of subsurface geothermal heat exchange fluid: CO_2 versus water and native brine. *Proceedings for the Geothermal Resources Council 35th Annual Meeting*: 23–26 Oct, 2011, San Diego, CA, USA.

Randolph, J.B., and Saar, M.O., 2011c. Combining geothermal energy capture with geologic carbon dioxide sequestration, *Geophysical Research Letters*, **38**, L10401, doi:10.1029/2011GL047265.

Randolph, J.B., 2013. Personal communication and spreadsheet on the thermal efficiency of a direct CO_2 turbine power system, University of Minnesota, Minneapolis, MN, USA.

Saar, M.O., Randolph, J.B., and Kuehn, T.H., 2010. Carbon Dioxide-based geothermal energy generation systems and methods related thereto. US Patent Application 20120001429.

Socolow, R.H. and Pacala, S.W., 2006. A plan to keep carbon in check, *Scientific American*, **295** (3), 50–57.

Span, R. and Wagner, W., 1996. A new equation of state for carbon dioxide covering the fluid region from the triple-point temperature to 1100K at pressures up to 800 MPa. *Journal of Physical and Chemical Reference Data*, **25**, 1509–1596.

van Genuchten, M.T., 1980. A closed form equation for predicting the hydraulic conductivity of unsaturated soils. *Soil Science Society of America Journal*, **44**, 892–898.

Zhou, Q., Birkholzer, J.T., Tsang C-F., and Rutqvist, J. A., 2008.A method for quick assessment of CO_2 storage capacity in closed and semi-closed saline formations. *International Journal of Greenhouse Gas Control*, **2**, 626–639.